

## EFFECTS OF IRON AND SILICON ON RECRYSTALLIZATION TEXTURES OF DRAWN ALUMINIUM

N. INAKAZU, Y. KANENO AND H. INOUE  
Department of Metallurgical Engineering,  
University of Osaka Prefecture,  
4-804, Mozu-Umemachi, Sakai, Osaka, 591, Japan.

### ABSTRACT

The recrystallization textures of cold drawn aluminium alloys were determined by means of the orientation distribution functions (ODFs). The changes in texture with annealing temperature were interpreted by examining the interrelation between recrystallization and precipitation. The drawing textures of all the specimens are mainly composed of the  $\langle 111 \rangle$  fiber component. In the case of Al-Si, silicon exists in the solid solution at high and medium temperatures (623-723K), therefore, the  $\langle 111 \rangle$  component is sharpened and the recrystallization textures are composed of the strong  $\langle 111 \rangle$  component and the weak  $\langle 100 \rangle$  one. On the other hand, precipitation of silicon participates in recovery and recrystallization at low temperatures (523-573K) so that the  $\langle 100 \rangle$  component nearly equals to the  $\langle 111 \rangle$  one in intensity. Al-Fe shows the strong  $\langle 111 \rangle$  + weak  $\langle 100 \rangle$  fiber texture in the all ranges of annealing temperatures, though the  $\langle 111 \rangle$  component is stronger at a high temperature (723K), where precipitation occurs after recrystallization, than at low and medium temperatures (573-673K), where it does before recrystallization. For Al-Fe-Si, the recrystallization textures are almost the same as Al-Fe except for weakening in orientation density.

### INTRODUCTION

It is known that the recrystallization textures of aluminium alloys are varied with annealing temperature - particularly, in case of precipitating during annealing<sup>1)</sup>. The recrystallization texture of cold rolled aluminium usually consists mainly of the cube orientation. However, R-texture which is similar to the

rolling texture is formed when the precipitation occurs during the recrystallization, because the fine particles of precipitates hinder the motion of the sub-boundaries and the dislocations<sup>2)</sup>. In this study, the recrystallization textures at various annealing temperatures were measured in drawn aluminium containing a slight amount of iron and silicon, and then an understanding of changes in fiber textures was acquired by clarifying the relation between recrystallization and precipitation.

## EXPERIMENTAL PROCEDURE

Five kinds of specimens, 99.9wt%Al, Al-0.05%Fe, Al-0.26%Fe, Al-0.11%Si and Al-0.27%Fe-0.11%Si, drawn to 90% reduction in area were isothermally annealed at 573K, 623K, 673K, 723K (in addition, 523K for Al-0.11%Si) in a salt bath. The process of recrystallization was investigated by means of the hardness measurements and the optical microscopic observations. The beginning of precipitation was determined by means of the electrical resistivity measurements. In addition, an electron microscope was used in order to observe both the microstructures and the precipitates. The texture measurements in the central region of specimens were carried out by the X-ray diffraction method. {111}, {200} and {220} pole figures were measured from which the three-dimensional orientation distribution functions (ODFs) were calculated by the series expansion method of Bunge's. Furthermore, the inverse pole figures were made from ODF data.

## EXPERIMENTAL RESULTS AND DISCUSSION

Figure 1 shows the variation of electrical resistivity with the isothermal annealing. In the case of Al-Si alloy, the electrical resistivity decreases gradually with the annealing temperature below 573K, while increases above 673K. It was found that the increasing of the electrical resistivity was due to resolution of silicon which was once precipitated by annealing or existed in the matrix before annealing, because the amount of precipitated silicon decreased from 0.018wt% to 0.002wt% with the annealing for 20s at 673K.

In the case of Al-Fe and Al-Fe-Si alloys, the electrical resistivity decreases in the all ranges of annealing temperatures but slightly at higher temperatures, because the solubility limit of Fe in Al is enlarged at higher temperatures.

Fiber texture in the drawn state consists mainly of the  $\langle 111 \rangle$  orientation component in all specimens<sup>3),4)</sup>, and the weak  $\langle 100 \rangle$  one is also found in 99.9%Al and Al-0.27%Fe-0.11%Si.

In all specimens, the  $\langle 111 \rangle + \langle 100 \rangle$  fiber texture is observed after the annealing. However, the fraction of the  $\langle 100 \rangle$  component to the  $\langle 111 \rangle$  one depends on both the alloying elements and the annealing temperature. The dependence of annealing temperature on recrystallization texture is roughly divided into two types.

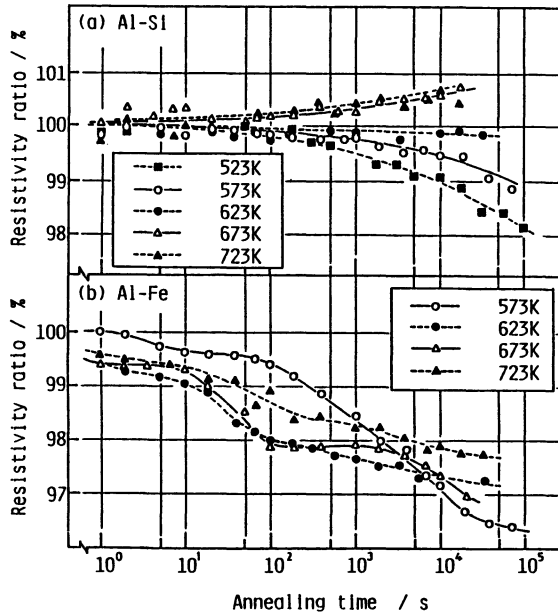


Figure 1 The variation of electrical resistivity ratio during the isothermal annealing, (a) Al-Si and (b) Al-Fe.

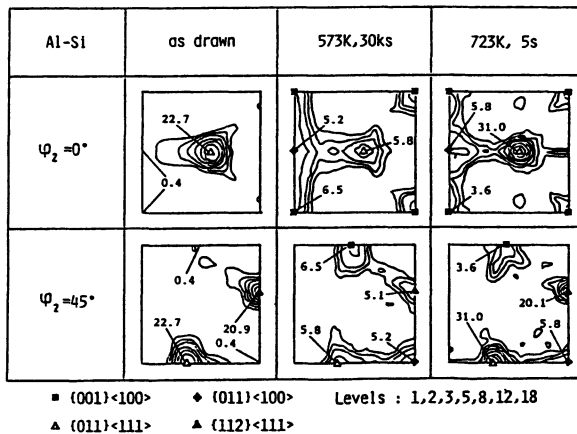


Figure 2 Drawing and recrystallization textures of Al-Si.

Figure 2 shows the  $\varphi_2=0$  and  $45^\circ$  sections of ODFs of Al-Si alloy. It is recognized that the  $\langle 111 \rangle$  fiber texture component increases in comparison with the deformed state by high (723K) and medium (623K, 673K) temperatures annealing and the  $\langle 100 \rangle$  component is stronger than the  $\langle 111 \rangle$  one by lower temperature ( $\leq 573$ K) annealing. 99.9%Al and Al-0.11%Si alloy belong to this type.

Figure 3, 4 show the ODFs of Al-Fe and Al-Fe-Si alloys. In the cases of both alloys, the  $\langle 111 \rangle$  component remains more strongly at a high temperature than that at medium and low temperatures. The specimens containing iron, Al-0.05%Fe, Al-0.26%Fe, Al-0.27%Fe-0.11%Si, belong to this type.

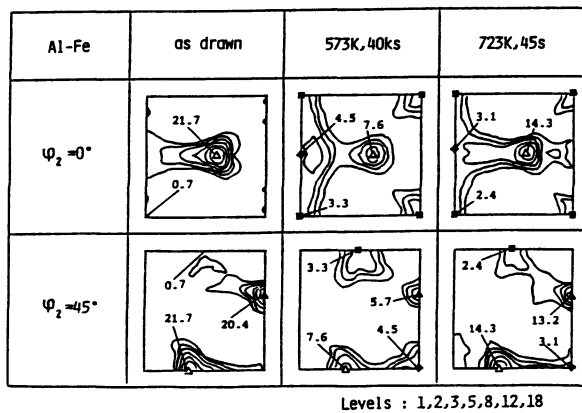


Figure 3 Drawing and recrystallization textures of Al-Fe.

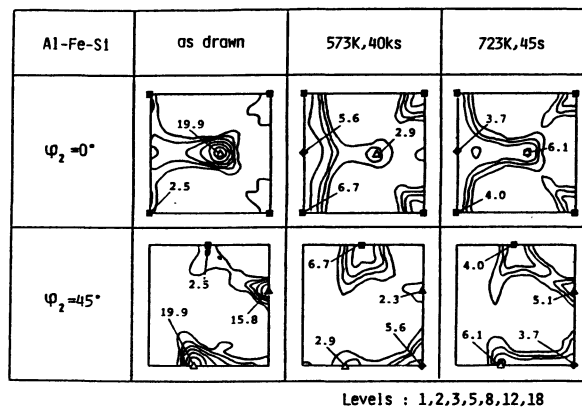


Figure 4 Drawing and recrystallization textures of Al-Fe-Si.

Figure 5 is the TTT diagrams showing the relation between recrystallization and precipitation. For Al-0.11%Si (Fig.5(a)), the recrystallization occurs independently on the precipitation at high and medium temperatures. Therefore, the  $\langle 111 \rangle$  fiber-texture component recovers and recrystallizes more preferentially than the  $\langle 100 \rangle$  one since the recrystallization is not suppressed by precipitation. Furthermore, it is supposed that the crystals with the near  $\langle 111 \rangle$  orientation rotate toward the stable  $\langle 111 \rangle$  one with the help of thermal activation. In the case of lower temperature, the precipitation occurs during the process of recovery or recrystallization. Therefore, it is considered that the  $\langle 100 \rangle$  component which is usually found in the recrystallization texture of aluminium increases, since the recovery and growth of the  $\langle 111 \rangle$  oriented sub-grains are suppressed due to hindering the migrating sub-boundaries by fine precipitates. But there is a difference between 99.9%Al and Al-0.11%Si. In the case of 99.9%Al, the precipitation does not occur even at lower temperature and hence the  $\langle 111 \rangle$  component remains strongly in comparison with Al-0.11%Si.

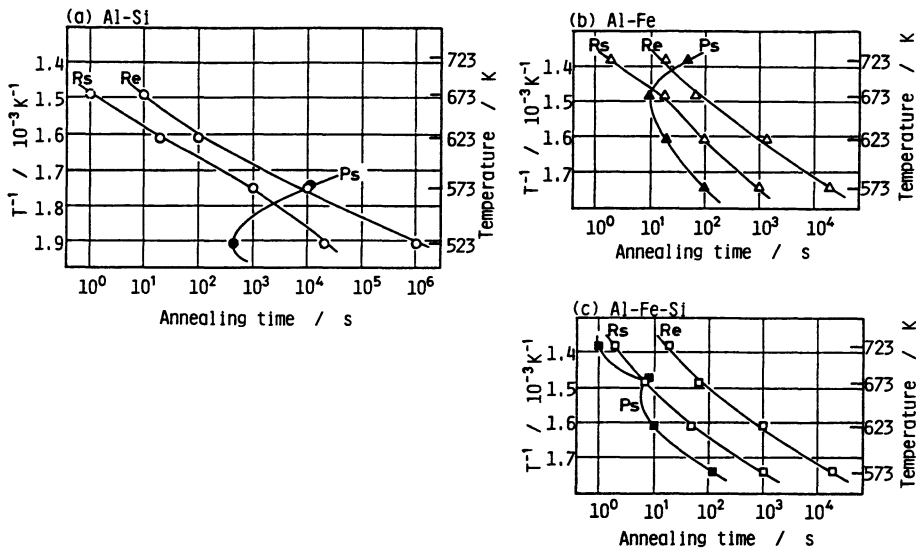


Figure 5 TTT diagrams for recrystallization and precipitation, (a) Al-Si, (b) Al-Fe and (c) Al-Fe-Si.

For Al-0.26%Fe (Fig.5(b)) and Al-0.05%Fe, as well as Al-0.11%Si, at low and medium temperatures, the precipitation occurs in the process of recovery (or the early stage of recrystallization), so that the  $\langle 111 \rangle$  fiber-texture component becomes weaker

than that at a high temperature where precipitation occurs after the recrystallization. Though the  $\langle 111 \rangle$  component, in Al-0.26%Fe, is stronger than the  $\langle 100 \rangle$  one at all ranges of temperatures. For Al-0.27%Fe-0.11%Si(Fig.5(c)), the precipitation occurs preferentially at all ranges of annealing temperatures. Therefore the  $\langle 111 \rangle$  fiber texture component becomes rapidly weaker than the  $\langle 100 \rangle$  one, and the  $\langle 100 \rangle$  component is stronger than the  $\langle 111 \rangle$  one at low and medium temperatures. From the consideration of the transmission electron micrographs and selected area diffraction patterns of Al-Fe annealed at 573K for 700s, it was recognized that the matrix was composed of two regions, that is, the  $\langle 100 \rangle$  and the  $\langle 111 \rangle$  components parallel to the drawing direction. The  $\langle 100 \rangle$  component region was composed of the microband accompanied with the large sub-grains, while the  $\langle 111 \rangle$  component region was surrounded by the small sub-grains. The matter mentioned above will interpret that the rate of recovery and grain growth in the  $\langle 100 \rangle$  region is faster than that in the  $\langle 111 \rangle$  region<sup>5)-7)</sup>.

## CONCLUSION

Compared with the deformed state, the  $\langle 111 \rangle$  fiber-texture component increases or remains strongly in the case of higher temperature annealing. In the case of lower temperature, the  $\langle 100 \rangle$  one increases and  $\langle 111 \rangle$  one decreases. But the  $\langle 111 \rangle$  one is further reduced if the precipitation occurs during the process of recovery or recrystallization. It is supposed that this may be attributed to the pinning effect by fine precipitates.

## REFERENCES

- 1) N. Inakazu and K. Lücke, *J.Japan Inst. Met.*, **49**, 921(1983).
- 2) N. Inakazu and Y. Kaneno, *J.Japan Inst. Met.*, **51**, 1116(1987).
- 3) H. Ahlborn and G. Wassermann, *Z.Metallkde.*, **54**, 496(1973).
- 4) N. Inakazu and H. Yamamoto, *J.Japan Inst. Met.*, **37**, 1224 (1973).
- 5) J. Huber and T. Noda, *Metall*, **32**, 571(1978).
- 6) T. Noda, J. Grewen and G. Wassermann, *Z.Metallkde.*, **67**, 450(1976).
- 7) H. Inoue, N. Inakazu and H. Yamamoto, *Proc. 6th. Int. Conf. Textures Mater.*, **1**, 591(1980).